

Supporting information

Inkjet deposition of liquid-exfoliated graphene and MoS₂ nanosheets for printed device applications

David J. Finn, Mustafa Lotya, Graeme Cunningham, Dave McCloskey, John F Donegan and Jonathan N. Coleman*

School of Physics, CRANN and AMBER, Trinity College Dublin, Dublin 2, Ireland

*colemaj@tcd.ie

Detailed methods section

Exfoliation of Graphene: Ink production

The graphene ink was obtained by sonicating pristine graphite in NMP. The graphite used was SGN-18 from FutureCarbon GmbH. ReagentPlus 99% grade NMP was purchased from Sigma Aldrich. An initial graphite concentration of 75 mg/ml was processed for 7 hours in 100 ml NMP using a horn tip sonicator (Sonics Vibra-cell VCX-750 ultrasonic processor) operating at 40% amplitude. The dispersion was processed inside a stainless steel flask with cooling provided by immersion in an ice water bath. This dispersion was then divided into two 50 ml portions and 50 ml of fresh NMP was added to each portion. These dispersion portions were then sonicated for a further 30 minutes at 70% amplitude. After sonication, the dispersion was then loaded into 14 ml glass vials and centrifuged using a Hettich Mickro 22R for 60 minutes at 3500 RPM. The top 12 ml of the dispersion was removed and centrifuged again under identical conditions. This procedure gives small graphene nanosheets dispersed at low concentration in a relatively large volume of NMP.

In order to raise the concentration of the graphene ink a third centrifugation step was performed. Four 10 ml Teflon centrifuge vials (Naglene Oakridge FEP centrifuge tubes) were filled to 9.3 ml volume and loaded in a Thermo Fisher Scientific Megafuge 16. The samples were centrifuged at 12000 rpm for 90 minutes. This process left a pale grey supernatant and a concentrated cluster of graphene flakes at the bottom of the vials. The supernatant was carefully extracted and discarded (concentration measured as 0.03 mg/ml). The concentrated graphene was then extracted by addition of a small amount of fresh NMP (approx. 0.5 ml). The contents of the four vials were combined and briefly sonicated in a bath sonicator to

redisperse the ink. UV-Vis spectrometry was used to measure $A_{660}/l = 26,100 \text{ m}^{-1}$ for the concentrated ink. Thus, the concentration of the ink was measured as $C_{\text{ink}} = 6.22 \text{ mg/ml}$, using the extinction coefficient of $4200 \text{ L mg}^{-1} \text{ mL}^{-1}$.

Optical absorbance measurements were carried out with a Varian Cary 6000i spectrometer using an optical glass cuvette having a cell length of 1 mm. The Lambert beer law relates absorbance (A) and length (l) to the concentration by: $A/l = \alpha C$ where α is the extinction coefficient and C is the concentration. The stock dispersion concentration was determined by measuring optical absorbance at 660 nm with reference to a previously determined extinction coefficient of $\alpha = 4200 \text{ L mg}^{-1} \text{ mL}^{-1}$. The stock dispersion had a measured $A_{660}/l = 2,192.9 \text{ m}^{-1}$, meaning a concentration of $C_{\text{stock}} = 0.52 \text{ mg/ml}$. This stock dispersion was found to be stable over several weeks.

Preliminary work using a similar procedure to the one outlined above yielded an ink concentration of approximately 1.5 mg/ml. This had been used to optimise jetting of the ink and to carry out print tests. In order to maintain consistency in the work, the concentrated ink was then diluted to 1.55 mg/ml. The thickness of the graphene flakes making up this ink was estimated using the TEM edge counting technique.¹ This involves the analysis of flake edges (figure S1, left) in order to estimate the number of monolayers per flake, N . By analysing 50 flakes, a histogram (figure S1, right) could be produced showing these flakes to contain 1-10 monolayers with a mean of $\langle N \rangle = 3.8$.

The obtained ink was syringe loaded into a cleaned print head cartridge and inkjet-printed on a selection of substrates. Inks more than two weeks old were briefly bath sonicated (20 minutes) in order to break up any aggregates or precipitates from the NMP dispersion, and to prevent clogging of the inkjet nozzles.

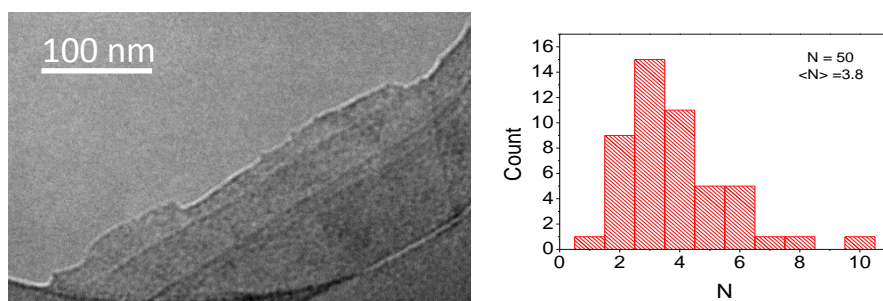


Figure S1: Left, example of flake edge showing monolayers. Right, flake thickness histogram.

Inkjet Printing

For experimental work, a Dimatix Materials Printer 2800 was used, a laboratory inkjet printer which uses a single printhead having 16 ejection nozzles (aperture: 21 μm) spaced 254 μm apart driven by piezoelectric elements jetting 10 picoliter droplets, and fed with the graphene/NMP based ink from a fluid bag encased in a plastic cartridge attached to the printhead. The graphene ink was obtained by sonicating pristine graphite in NMP. Mild centrifugation was used to remove large unexfoliated material and large flakes, with subsequent high rotation rate centrifugation steps used to produce a concentrated ink suitable for inkjet printing.

The jetting channels of the 16 piezoelectric elements expand or contract when a bias voltage is applied, thus creating a propagating pressure wave at each nozzle, propelling tiny droplets of functional ink to jet, after overcoming the surface tension and viscous forces of the fluid.²

The operating parameters of the jetting droplets from each nozzle, controlling drop volume, drop shape and formation, need to be tailored to minimize tails and satellites. These parameters affecting drop formation include: drop velocity, piezo driving waveform shape and duration, viscosity, density and surface tension of the ink, as well as the shape and size of the nozzles. Viscosity has a major impact on the formation of tails and their viscous length, whereas high concentration results in shorter tails. Congested nozzles disturb enormously the shape and trajectory of the ejected droplets.²

Strategies to mitigate the effect of nozzle clogging (insufficient firing of the nozzles during operation, results in evaporation of the solvent at the orifice of the nozzle and leads to the build-up of solid material inside and around the nozzle rim) were implemented during every printing routine. For example, the jetting performance of each nozzle was monitored during and after printing, observing the jetted drops by strobe illumination in the drop watcher.

The substrate was placed on a vacuum platen which can be heated to 60 °C. The temperature of the fluid in the printhead can be raised above ambient (max. 70 °C) to lower the viscosity and to optimize the desired jetting performance. The NMP solvent in the jetted droplets should evaporate on contact with the heated substrate. However, the evaporation kinetics of the solvent vehicle are dependent on the surface energy of the substrate, surface tension of the ink, substrate temperature, ink temperature, absorption, spreading and the thickness of the

substrate. Attempts to print on untreated silicon substrates proved unsuccessful with coagulation of the ink droplets on the surface and non-uniform drying, this effect has been previously noted in the literature.³ Poor drying was also observed on untreated PET. We tested a number of substrates and found an optimum with a semi-transparent coated PET material from Mitsubishi Paper Mills Ltd, NB-TP-3GU100. This material consisted of a coating of aluminium oxide and polyvinyl alcohol on PET and is generally intended for use in the inkjet printing of water-based silver nanoparticle ink.

During experimental trials a number of significant challenges were faced printing conductive features through multiple inkjet passes on the coated PET substrate, followed by permeation and evaporation of the solvent vehicle on the substrate, and after drying, the graphene content of the ink forming a uniform pattern with good electrical properties.

Visible striations or swathe lines running parallel the printhead raster direction impaired the quality and uniformity of the printed conductive lines. This non-uniformity ultimately limits the electrical conductivity of the printed line, with the conductivity defined by the thinnest regions. Tuning the properties of the solvent vehicle to match the wetting properties of the substrate can reduce significantly the presence of swathe lines, with further research emphasis on solvent selection, blending and using different solvents for different stages in the graphene-ink production process.

To measure the thickness of an array of graphene printed traces on a transparent substrate with each trace having a different number of inkjet passes, a positive film image was taken of the entire substrate recorded using a 48-bit RGB colour depth and 6400 dpi resolution (spatial resolution of 4 μm). Data was saved in TIFF format. The scanned images of the transparent substrate with and without graphene traces were imported into Origin for numeric computation. The imported data was converted from signal intensity to transmittance using a polynomial calibration fit. This transmittance data was subsequently converted to absorbance.

Interdigitated Graphene Electrode Array

An interdigitated graphene electrode array was printed on coated PET. The graphene electrodes were fabricated in a structure as shown in Figure S2, having a finger width of 1 mm, electrode gap of 1 mm and electrode length of 20 mm. The graphene electrodes were made to an estimated thickness of 215 nm using 10print passes with an ink at 1.5 mg/ml concentration.

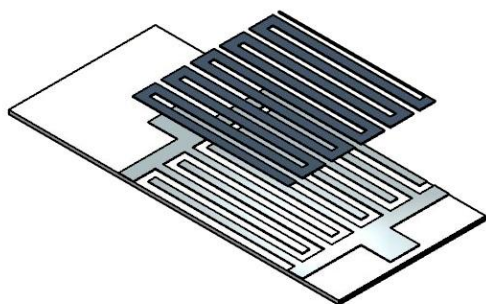


Figure S5: Exploded diagram of final electrode array with MoS₂ filler

Comparison to literature

ref	Graphene type	anneal	Best electrical performance
This work	NMP exfoliated graphene	70 C during print	$\sigma=3000$ S/m
Secor ⁴	Liquid exfoliated graphene	250 C for 30 min	$\sigma=25000$ S/m
Li ⁵	Liquid exfoliated graphite (DMF)	375-400 C for 0.5-1hr mins	$R_s=40$ kOhm/sq (T=77%) [$\sigma\sim 3400$ S/m*]
Kong ⁶	RGO	~ 200 C 10 min (heat lamp)	$R_s=0.3$ MOhm/sq (T=86%) [$\sigma\sim 800$ S/m*]
Lim ⁷	RGO	350 C	$\sigma=70$ S/m
Torrise ³	Liquid exfoliated graphite	170 C for 5 min	$\sigma=100$ S/m
Huang ⁸	RGO	400 C for 3 hrs**	900 S/m
Shin ⁹	RGO	90 C in hydrazine	$R_s=65$ Ohm/sq $\sigma\sim 3.5e4$ S/m
Le ¹⁰	RGO	200 C	NA
Shin ¹¹	RGO	90 C in hydrazine	$\sigma=5500$ S/m
Dua ¹²	RGO	80 C	$\sigma=15$ S/cm

*Calculated from R_s , T data using $T = \left[1 + \frac{Z_0}{2R_s} \frac{\sigma_{op}}{\sigma_{DC}} \right]^{-2}$ assuming $\sigma_{op} = 1 \times 10^5$ S/m.¹³

** Personal communication from author

References

- (1) Khan, U.; O'Neill, A.; Lotya, M.; De, S.; Coleman, J. N. High-Concentration Solvent Exfoliation of Graphene. *Small* **2010**, *6*, 864-871.
- (2) Wijshoff, H. Structure- and Fluid-Dynamics in Piezo Inkjet Printheads, University Twente, 2008.
- (3) Torrisi, F.; Hasan, T.; Wu, W. P.; Sun, Z. P.; Lombardo, A.; Kulmala, T. S.; Hsieh, G. W.; Jung, S. J.; Bonaccorso, F.; Paul, P. J. et al. Inkjet-Printed Graphene Electronics. *Acs Nano* **2012**, *6*, 2992-3006.
- (4) Secor, E. B.; Prabhumirashi, P. L.; Puntambekar, K.; Geier, M. L.; Hersam, M. C. Inkjet Printing of High Conductivity, Flexible Graphene Patterns. *Journal of Physical Chemistry Letters* **2013**, *4*, 1347-1351.
- (5) Li, J.; Ye, F.; Vaziri, S.; Muhammed, M.; Lemme, M. C.; Ostling, M. Efficient Inkjet Printing of Graphene *Advanced Materials* **2013**, *25*, 3985-3992.
- (6) Kong, D.; Le, L. T.; Li, Y.; Zunino, J. L.; Lee, W. Temperature-Dependent Electrical Properties of Graphene Inkjet-Printed on Flexible Materials. *Langmuir* **2012**, *28*, 13467-13472.
- (7) Lim, S.; Kang, B.; Kwak, D.; Lee, W. H.; Lim, J. A.; Cho, K. Inkjet-Printed Reduced Graphene Oxide/Poly(Vinyl Alcohol) Composite Electrodes for Flexible Transparent Organic Field-Effect Transistors. *Journal of Physical Chemistry C* **2012**, *116*, 7520-7525.
- (8) Huang, L.; Huang, Y.; Liang, J. J.; Wan, X. J.; Chen, Y. S. Graphene-Based Conducting Inks for Direct Inkjet Printing of Flexible Conductive Patterns and Their Applications in Electric Circuits and Chemical Sensors. *Nano Research* **2011**, *4*, 675-684.
- (9) Shin, K. Y.; Hong, J. Y.; Jang, J. Micropatterning of Graphene Sheets by Inkjet Printing and Its Wideband Dipole-Antenna Application. *Advanced Materials* **2011**, *23*, 2113-+.
- (10) Le, L. T.; Ervin, M. H.; Qiu, H. W.; Fuchs, B. E.; Lee, W. Y. Graphene Supercapacitor Electrodes Fabricated by Inkjet Printing and Thermal Reduction of Graphene Oxide. *Electrochemistry Communications* **2011**, *13*, 355-358.
- (11) Shin, K. Y.; Hong, J. Y.; Jang, J. Flexible and Transparent Graphene Films as Acoustic Actuator Electrodes Using Inkjet Printing. *Chemical Communications* **2011**, *47*, 8527-8529.
- (12) Dua, V.; Surwade, S. P.; Ammu, S.; Agnihotra, S. R.; Jain, S.; Roberts, K. E.; Park, S.; Ruoff, R. S.; Manohar, S. K. All-Organic Vapor Sensor Using Inkjet-Printed Reduced Graphene Oxide. *Angewandte Chemie-International Edition* **2010**, *49*, 2154-2157.
- (13) De, S.; Coleman, J. N. Are There Fundamental Limitations on the Sheet Resistance and Transmittance of Thin Graphene Films? *Acs Nano* **2010**, *4*, 2713-2720.